JGR Atmospheres

RESEARCH ARTICLE
10.1029/2025JD043318

Climate Offsets CO_2 Increase as the Main Driver of Tree Growth in Arid and Semi-Arid Northern China

Tao Yang[1], Bao Yang[2], Shuangjuan Wang[2], Étienne Boucher[3], Sergio Rossi[4,5], Ignacio Hermoso[3], and Timothy J. Osborn[6]

[1]College of Urban Rural Planning and Architectural Engineering, Shangluo University, Shangluo, China, [2]School of Geography and Ocean Science, Nanjing University, Nanjing, China, [3]Dépt. de géographie, GEOTOP and Centre d'études Nordiques, Université du Québec à Montréal, Montreal, QC, Canada, [4]Département des Sciences Fondamentales, Université du Québec à Chicoutimi, Chicoutimi, QC, Canada, [5]Key Laboratory of Vegetation Restoration and Management of Degraded Ecosystems, Guangdong Provincial Key Laboratory of Applied Botany, South China Botanical Garden, Chinese Academy of Sciences, Guangzhou, China, [6]Climatic Research Unit, School of Environmental Sciences, University of East Anglia, Norwich, UK

Key Points:

- Climate change rather than CO_2 fertilization plays a dominant role in controlling tree growth in arid and semi-arid northern China
- Intrinsic water-use efficiency has been significantly enhanced, but has not translated into increased tree growth
- Ongoing climatic trends will likely increase tree growth in arid region, but decrease growth rates in semi-arid region

Supporting Information:

Supporting Information may be found in the online version of this article.

Correspondence to:

B. Yang,
yangbao@nju.edu.cn

Citation:

Yang, T., Yang, B., Wang, S., Boucher, É., Rossi, S., Hermoso, I., & Osborn, T. J. (2025). Climate offsets CO_2 increase as the main driver of tree growth in arid and semi-arid northern China. *Journal of Geophysical Research: Atmospheres*, *130*, e2025JD043318. https://doi.org/10.1029/2025JD043318

Received 3 MAR 2025
Accepted 20 SEP 2025

Author Contributions:

Conceptualization: Tao Yang, Bao Yang
Data curation: Bao Yang
Funding acquisition: Bao Yang
Investigation: Tao Yang, Bao Yang
Methodology: Tao Yang, Bao Yang, Étienne Boucher, Sergio Rossi, Ignacio Hermoso, Timothy J. Osborn
Resources: Bao Yang
Supervision: Bao Yang
Visualization: Tao Yang, Shuangjuan Wang
Writing – original draft: Tao Yang, Bao Yang
Writing – review & editing: Tao Yang, Bao Yang, Étienne Boucher, Sergio Rossi, Ignacio Hermoso, Timothy J. Osborn

Abstract The combined contribution of CO_2 fertilization and climate variability to arid and semi-arid forest growth remains unclear. To disentangle these multiple influences, we used a preexisting process-based ecophysiological model (MAIDENiso) to simulate tree growth changes during 1956–2010 in arid and semi-arid regions of China. Results revealed that simulated tree growth was more dependent on climate trends than on atmospheric CO_2 concentration. Mechanistic analysis showed that the regulation of stomatal conductance under water stress positively affected tree growth in the arid region, but had an opposite pattern in the semi-arid region. Intrinsic water-use efficiency (iWUE, measured from tree-ring $\delta^{13}C$) has increased by 29% and 44% since 1900 CE in the arid and semi-arid regions, respectively, but did not stimulate radial tree growth. This suggests that there will possibly be a continued increase (decrease) of radial forest growth in arid (semi-arid) areas of northern China if the current climate trends remain in the next decades.

Plain Language Summary The atmospheric CO_2 concentration has increased rapidly since 1850. It is difficult to identify CO_2-related impacts on tree growth without separating them from those associated with climate variability. Here, we modeled these confounding effects with a numeric tree-ring model of the ecological and physiological controls on tree growth. We found that, since 1956, the contribution of climate (water stress) to radial tree growth has been more important than elevated CO_2 in arid and semi-arid regions of northern China. In addition, results also showed that the intrinsic water use efficiency derived from tree-ring $\delta^{13}C$ increased significantly, but did not increase radial tree growth in our study regions. Therefore, we conclude that tree radial growth rates will increase in the near future if the climate gets wetter, or will decrease if the climate gets significantly drier, even if CO_2 continues to rise.

1. Introduction

Human activities, especially the rapid consumption of fossil fuels following the industrial revolution, have increased atmospheric CO_2 concentrations, which are the major drivers of current global warming (Flato et al., 2013). Forests, as substantial terrestrial carbon pools and crucial components of the global carbon cycle, play an intrinsic role in the coupled changes of climate and carbon cycles because they respond to both atmospheric CO_2 concentration and regional climate changes (Cernusak et al., 2013; Girardin et al., 2016; Pan et al., 2011; Silva et al., 2016; Sleen et al., 2015). However, these responses are only understood in broad terms: warming and rise in atmospheric CO_2 concentration affect the processes of carbon fixation, transport and organic synthesis during plant photosynthesis (Ainsworth & Rogers, 2007), as well as impacting forest dynamics, including tree-line expansion, lengthening of the growing season, and increasing forest mortality (Harsch et al., 2009; Williams et al., 2013; Yang et al., 2017). More research is needed to quantify the details of these responses, especially when they are accompanied by aridity changes.

Enormous research efforts have been made to assess the effects of CO_2 "fertilization" by means of controlled experiments, which include a replication of the study under defined growing conditions. Results for more than 40 species in 12 free-air CO_2 enrichment (FACE) sites suggest that trees increase their responses to CO_2 concentration and leaf area index (LAI) more than other functional groups (Ainsworth & Long, 2005). Nevertheless,

these experiments have limitations: first, most of them studied individual species grown in enclosed systems, different from natural forests (Ainsworth & Long, 2005); second, the relatively short (only a few years) duration of these experiments hampers efforts to determine the response of tree growth to elevated CO_2 concentration over longer (decadal to multi-decadal) time scales (Babst et al., 2014).

In recent years, dendrochronology has become an important tool to understand the response of trees to changing atmospheric CO_2 concentration on long time scales (Girardin et al., 2016; Lavergne et al., 2019; Marchand et al., 2020; Panthi et al., 2019; Silva et al., 2016; Sleen et al., 2015; Zuidema et al., 2020). These studies have undoubtedly contributed to the exploration of the effects of carbon dioxide on tree growth over long timescales. However, the methods used in these studies have revealed some limitations (Giguère-Croteau et al., 2019; Girardin et al., 2016; Sleen et al., 2015; Wang et al., 2019). On one hand, the relationships between growth and CO_2 have been traditionally detected on a statistical basis, that is, linear models (Wang et al., 2019) and linear mixed models (Panthi et al., 2019; Sleen et al., 2015), which are not able to disentangle the effects of CO_2 from those biological processes on tree growth, and to capture the non-linear processes. On the other hand, process-based models (Vaganov-Shashkin and Vaganov-Shashkin-Lite) have successfully assessed the effects of climate on tree growth and growing season length (Peng et al., 2019; Tolwinski-Ward et al., 2010; Yang et al., 2017), but CO_2 concentration was often excluded from the environmental factors involved in the system. Therefore, it is impossible to detect the influence of atmospheric CO_2 concentration with such models. The ecophysiological model MAIDENiso (Danis et al., 2012) provides a framework to simulate the influence of both climate and CO_2 on photosynthesis, phenology and carbon allocation through ecophysiological equations and mechanistic rules, which could give us an opportunity to separate the contributions of CO_2 and climate change to forest growth in a long-term and mechanistic perspective (Gea-Izquierdo et al., 2015; Gennaretti et al., 2017).

Forests in arid and semi-arid northern China play an important role in preserving the ecological environment. The forest ecosystem exhibits low biodiversity in such areas due to low annual precipitation, and is therefore particularly sensitive to ongoing climate change, especially during drought periods (Liang et al., 2006; Qin et al., 2025; Yang, Kang, et al., 2014; Yang, Qin et al., 2014; Yang et al., 2023). Disentangling the influence of enhanced CO_2 and climate change on tree growth in these regions from a mechanistic perspective is of great importance in projecting forest growth rate but remains unresolved (Huang et al., 2016). In this study, we use the tree-ring model MAIDENiso to investigate how tree growth in arid and semi-arid forests (Zheng et al., 2013) has been modified by the combined effects of climate and CO_2 concentrations over the last six decades. We tested the hypothesis that tree growth in these regions is driven by water stress.

2. Material and Methods

2.1. Tree-Ring Data Collection and Chronology Development

Two different climatic regions were studied, Zongwulong Mountain (37°27′N, 97°47′E, 3,700–4,000 m a.s.l.) in Delingha and Hasi Mountain (37°02′N, 104°28′E, 2,400–2,700 m a.s.l.) in Jingyuan. The mean annual temperatures were around 3.9°C and 9.1°C in Delingha and Jingyuan from 1956 to 2014, with the coldest and warmest months being January and July, respectively. Total annual precipitation was 174 and 234 mm, respectively, with about 70% concentrated in summer (Figure S1 in Supporting Information S1). Based on the amount of precipitation, Delingha and Jingyuan are classified as arid and semi-arid areas, respectively (Figure S2 in Supporting Information S1).

The dominant tree species in the arid region is Qilian juniper (*Sabina przewalskii* Kom.) on a south-facing slope, and Chinese pine (*Pinus tabuliformis*) on a north-facing slope in the semi-arid region. The tree-ring samples were collected at breast height (1.3 m) with an increment borer. For each tree, one to two increment cores were taken from different directions. In total, 361 cores from 208 trees and 282 cores from 141 trees were collected in arid and semi-arid regions, respectively. These tree-ring samples were processed using standard dendrochronological techniques (Stokes & Smiley, 1968). All the increment cores were air dried and sliced with razor blades until distinct tree rings were visible under a microscope. Each ring width was recorded using LINTAB 6 measuring system at a resolution of 0.01 mm. The tree-ring width series were cross-dated with TSAP-Win. Furthermore, the accuracy of ring width measurements and crossdating were detected by program COFECHA (Holmes, 1983). The standard chronology in both regions (Figure 1) were ultimately detrended with negative exponential curves to remove age-related biological trends by using ARSTAN software (Cook, 1985) (Figure S3 and Table S2 in Supporting Information S1). We recognize that tree-ring width varies with cambial age, a process named tree

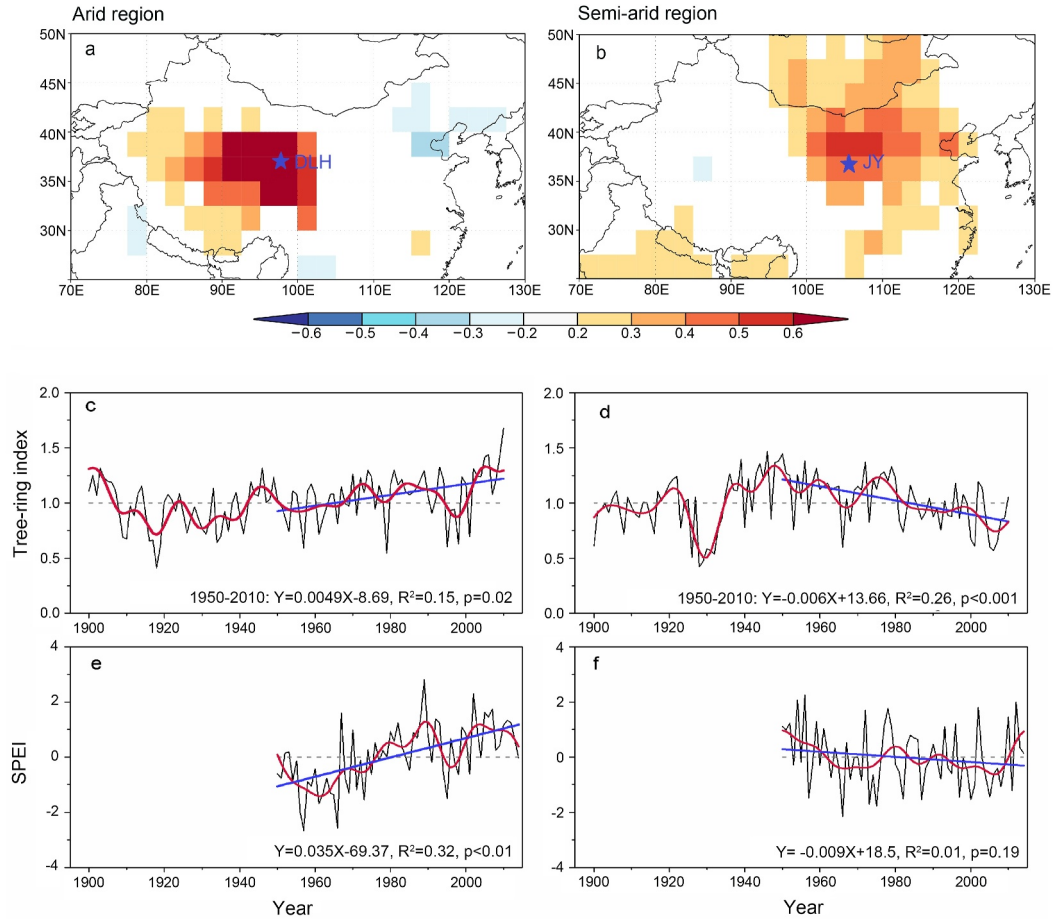

Figure 1. Map of the study area, showing the tree-ring sampling sites (DLH, Delingha the arid region; JY, Jingyuan the semi-arid region); (a, b). Spatial correlations between tree-ring width and reconstructed Palmer Drought Severity Index (PDSI) (Cook et al., 2010) are shown in panels (a) and (b). Tree-ring width chronologies and June–August (12-month scale) mean Standardized Precipitation-Evapotranspiration Index (SPEI, Text S1a in Supporting Information S1), together with their 10-year low-pass filtered variations (red) and linear trends since 1950 (blue), are shown for arid (c, e) and semi-arid (d, f) regions.

growth trend, which follows a negative exponential pattern. This method is primarily used to remove non-climatic trends caused by age-related growth or environmental changes while gently suppressing low-frequency signals, thereby better preserving the information related to long-term climatic trends. Moreover, since the influence of non-climatic factors on trees in our study area is marginal, we applied the negative exponential method to detrend the tree-ring width chronology. To detect the potential effects associated with the detrending method, we employed the signal-free negative exponential approach to develop the tree-ring chronology at each study site for comparison. The results revealed that these chronologies demonstrate a high degree of similarity from 1750 to 2010 (Figure S4 in Supporting Information S1). Based on these findings, we proceeded with the negative exponential method-derived chronologies for the subsequent analyses. Even if restricted to geographic area, our tree ring chronologies are significantly correlated with chronologies from adjacent regions (Figure S5 in Supporting Information S1). This allowed us to use these chronologies to assess tree-growth variability in northern China.

We selected 10 and 9 individual increment cores from the arid and semi-arid regions, respectively, for analyzing stable isotope components of tree-ring cellulose (Table S3 in Supporting Information S1). The cores selected were those with clear ring boundaries, and without breaks or missing rings. We pooled samples of the same calendar year from different tree samples. Samples from the two regions were all at annual resolution (Figure S6 in Supporting Information S1). These pooled samples were ground in a mill and the α-cellulose extraction process

described by Wieloch et al. (2011) was conducted in the isotope laboratory of the Institute of Geography at University of Erlangen-Nuremberg, Germany. We measured tree-ring $\delta^{13}C$ values with an on-line mass spectrometer (Delta V Advantage, Thermo Scientific, Bremen, Germany). The analytical errors of the isotope measurements were less than 0.25‰.

2.2. Definitions and Equations for the Tree Ring Carbon Isotopes

The variation of tree iWUE is an important indicator reflecting ambient conditions and is expressed (Farquhar et al., 1982) as the ratio of photosynthetic assimilation rate (A) to stomatal conductance (g_s) for water vapor:

$$iWUE = \frac{A}{g_s} = \frac{C_a - C_i}{1.6} = \frac{C_a\,(1 - C_i/C_a\,)}{1.6} \tag{1}$$

where C_i and C_a are intercellular and atmospheric CO_2 concentrations. The ratio C_i/C_a, is related to, and can be calculated from the carbon isotope discrimination ($\Delta^{13}C$) value in the plant:

$$\Delta^{13}C = a + (b - a)\,C_i/C_a \tag{2}$$

where $a = 4.4‰$ (McCarroll & Loader, 2004) is the discrimination value for the process of CO_2 diffusion from the air into the leaf cells and $b = 27‰$ (McCarroll & Loader, 2004) is the discrimination value for carboxylation. Carbon isotope discrimination is determined (Saurer et al., 2004) as follows:

$$\Delta^{13}C = \frac{\delta^{13}C_a - \delta^{13}C_p}{1 + \delta^{13}C_p/1000} \tag{3}$$

where $\delta^{13}C_a$ (McCarroll & Loader, 2004) and $\delta^{13}C_p$ are the stable carbon isotope ratio of atmospheric CO_2 and tree ring cellulose, respectively.

Fossil fuel burning has contributed to the increase in atmospheric CO_2 concentration and reduced its stable carbon isotope ratio by ~1.8‰ since the beginning of the industrial era (McCarroll & Loader, 2004). This decline in $\delta^{13}C_a$ influences the tree-ring stable carbon isotopes (which show a downward trend in recent decades: Figure S6 in Supporting Information S1), therefore, before extracting the climatic signals, we removed this influence from the raw tree ring $\delta^{13}C_p$ series. However, before the Industrial Revolution, the concentration of CO_2 in the atmosphere changed only slightly, generally ranging between 260 and 285 ppm. Therefore, the $\delta^{13}C$ value in the atmosphere also remained basically stable at −6.4‰ before this period (McCarroll & Loader, 2004):

$$\delta^{13}C_{cor} = \delta^{13}C_p - \left(\delta^{13}C_a + 6.4\right) \tag{4}$$

2.3. The MAIDENiso Model

MAIDENiso (Danis et al., 2012) explicitly includes several ecophysiological processes, such as photosynthesis, respiration, carbon allocation, and water allocation, to simulate tree productivity. This model captures the influence of meteorological variables and atmospheric CO_2 concentration on tree growth through explicit equations and rules. MAIDENiso simulates photosynthesis at a daily scale and allocates carbon to different tree compartments (leaf, root, stem, and storage) based on five phenological phases during each year. Those phases are: (a) tree dormancy during a winter period, where all photosynthates are allocated to a storage reservoir; (b) leaf and root expansion in spring during the accumulation of growing degree days; (c) bole wood production during summer, when carbon is allocated to roots, stem, and canopy; (d) carbohydrate reserve accumulation during fall, when photosynthates are allocated to bole and non-structural carbohydrates; (e) leaf and root senescence, which starts when the photoperiod is less than a minimum threshold (see more details in Text S1b of Supporting Information S1). At the end of each year, all carbon allocated to the stem represents the annual tree growth increment, which is assumed to be proportional to tree-ring width (Gea-Izquierdo et al., 2015).

There are 6 parameters controlling gross primary production (GPP) and 12 parameters influencing the daily carbon from photosynthesis allocated to tree stem, and they are optimized by a Bayesian procedure with Markov Chain Monte Carlo (MCMC) sampling using Metropolis-Hasting steps. Details of the calibration process are

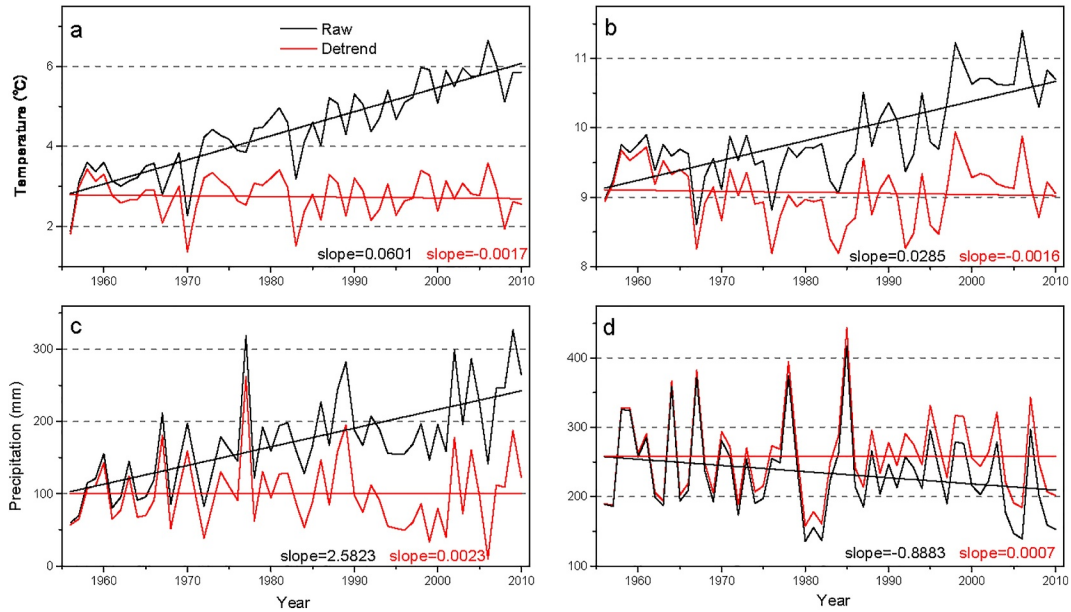

Figure 2. Variations of mean annual temperature and annual total precipitation for raw and detrended data in the arid (left) and semi-arid (right) regions during the period 1956–2010. The slope (°C/year or mm/year) of each regression line for raw and detrended data is also labeled.

described in Gennaretti et al. (2017). First, we calibrate the 6 parameters linked with photosynthesis to maximize the coherence on a daily scale between simulated and GPP measured from an eddy covariance station for the years 2010 and 2011 (Figure S7 in Supporting Information S1). Second, the 12 parameters affecting bole increment were optimized by comparing the yearly bole increment from 1956 to 2010 with measured tree-ring width chronologies. We ran 50 Markov chains each time with random initial values in their prior ranges to verify the convergence of MCMC sampling. The highest model posterior probability of each chain was retained. The calibrated values for those parameters that most strongly control the simulated GPP and carbon allocation are shown in Table S4 of Supporting Information S1.

The input data of the MAIDENiso model are the maximum and minimum daily air temperature, precipitation, and atmospheric CO_2 concentration (Text S1c in Supporting Information S1). We ran three model experiments under these inputs: (a) all daily temperature, precipitation and CO_2 concentration correspond to actual observations (hereafter RAW); (b) weather variables correspond to those observed, whereas CO_2 concentration stays with the 1956 value (hereafter CO_{2FIX}); (c) weather variables are linearly detrended, and the observed timeseries of CO_2 is used (without detrending) (hereafter $MET_{DETREND}$, Figure 2). The representativeness of the input data was validated using CN05.1 (Wu & Gao, 2013) and ERA5 data sets (Muñoz Sabater, 2019) (Text S1f of Supporting Information S1). We use the "detrend" function in MATLAB to remove the linear trend of daily temperature and precipitation in both study regions. Firstly, we performed linear regression on the original mean annual temperature and precipitation in the two study regions, respectively. The significance of the linear trends was assessed by analysis of variance (ANOVA). Then, based on the linear equations, the temperature and precipitation values for each year were calculated. Finally, the detrended sequences were obtained by subtracting the sequences calculated from the fitted equations from the original sequences (Figure 2).

During the simulation process, we required parameters related to tree species and their external environmental conditions, such as soil texture, water content, and leaf area index (Misson, 2004a, 2004b) (Text S1d of Supporting Information S1). For *Pinus tabuliformis* and *Sabina przewalskii*, we assigned simulation parameters by referring to extensive previous research (Wu & Xing, 2015; Zhao, 2009). Additionally, observational data regarding phenological changes of these species at the study sites were obtained based on published observational data (Gao, 2021; Ren et al., 2018; Yang, Kang et al., 2014; Yang, Qin et al., 2014; Zeng, 2017).

Table 1
Correlation Coefficients Between Measured Tree-Ring Width and Bole Increment Simulated by MAIDENiso Model Under Different Experiments During 1956–2010

Study site	Experiment	Pearson correlation	First-order difference[a]
Arid region	RAW	0.71 ($p < 0.01$)	0.66 ($p < 0.01$)
	CO_{2FIX}	0.70 ($p < 0.01$)	0.65 ($p < 0.01$)
	$MET_{DETREND}$	0.51 ($p < 0.01$)	0.51 ($p < 0.01$)
Semi-arid region	RAW	0.46 ($p < 0.01$)	0.57 ($p < 0.01$)
	CO_{2FIX}	0.53 ($p < 0.01$)	0.52 ($p < 0.01$)
	$MET_{DETREND}$	0.26 ($p > 0.01$)	0.57 ($p < 0.01$)

[a]First-order difference series were calculated using the data of each year minus its previous year, effectively removing their tree growth trends, before calculating the correlation coefficients. The significant coefficients of both Pearson and first-order difference results revealed that our simulated results were reliable.

3. Results

3.1. Comparison Between Measured and Simulated Tree Growth

Our tree-ring measurements from 1950 to 2010 exhibit a significant ($P < 0.05$) increasing trend of tree growth in the arid region, whereas a downward trend was observed in the semi-arid region (Figure 1). When driven by observed meteorological variables and atmospheric CO_2, MAIDENiso predicts comparable growth trends in both regions. The interannual variability in tree-growth is also well simulated, with correlations between simulated and measured tree growth of 0.71 ($P < 0.01$) for the arid region and 0.46 ($P < 0.01$) for the semi-arid region (Table 1). The strong relationships between observed and simulated tree-ring width (including for first-order differences: Table 1) indicate that MAIDENiso performs well in both study regions. Running MAIDENiso with constant, rather than time-varying, atmospheric CO_2 concentrations barely alters the correlations between simulated and measured tree growth indices (Table 1). However, driving MAIDENiso with detrended temperature and precipitation (Figure 2) weakens the correlations with observed tree ring widths for arid ($r = 0.51$, $P < 0.01$) and semi-arid regions ($r = 0.26$, $P > 0.01$) (Table 1). This suggests that trends in tree growth, as well as its interannual variability, are more sensitive to climatic drivers than to CO_2 concentration.

The growth trends simulated by MAIDENiso are driven by trends in the input data (temperature, precipitation, and CO_2). The linear trends of simulated bole increment were close to trends in tree-ring chronologies (nonsignificant differences were found between the slopes) in both study regions (Figures 3a and 3b). In both regions, the commonality analysis was used to assess the contribution of climatic factors and CO_2 on tree growth (Text S1e in Supporting Information S1). From 1956 to 2010, the total variance in arid region was 23.8%, of which the pure effects of temperature, precipitation, and CO_2 on tree growth were 0.01%, 8.8%, and 0.2%, respectively (Table S5 in Supporting Information S1). Holding CO_2 constant (CO_{2FIX}) reduces the simulated trend by 50% (from 0.75 to 0.37 g C m^{-2} yr^{-1}; Figure 3c), whereas detrending the meteorological inputs changes the trend from 0.75 to −0.06 g C m^{-2} yr^{-1}. These effects are clear in the individual experiments (Figure 3c) and especially in the residuals between RAW and the other experiments (Figure 3e). In the semi-arid region, 30.1% of the total variance in tree growth can be explained by temperature (2.3%), precipitation (1.5%), and CO_2 (4.5%) (Table S5 in Supporting Information S1). In addition, we found the decreasing growth trend in RAW was enhanced in the CO_{2FIX} experiment, whereas it is mostly removed in the $MET_{DETREND}$ experiment which simulated higher bole increment than RAW especially since 1983 (Figure 3d). The residuals between RAW and the other experiments (Figure 3f) show that the contribution to the simulated bole increment trend caused by CO_2 is smaller in magnitude than the effect of the climatic trends. The slopes were 0.38 and 0.82 g C m^{-2} yr^{-1} for the arid region, with the mean value of bole increment 7.71 and 25.69 g C m^{-2} (Figure 3e). In the semi-arid region, the trends caused by CO_2 and climate were 0.19 and −0.18 g C m^{-2} yr^{-1}. Although the slopes were similar, we can still find a higher mean value of bole increment caused by climate (−7.35 g C m^{-2}) than CO_2 (4.29 g C m^{-2}) during 1956–2010 (Figure 3f).

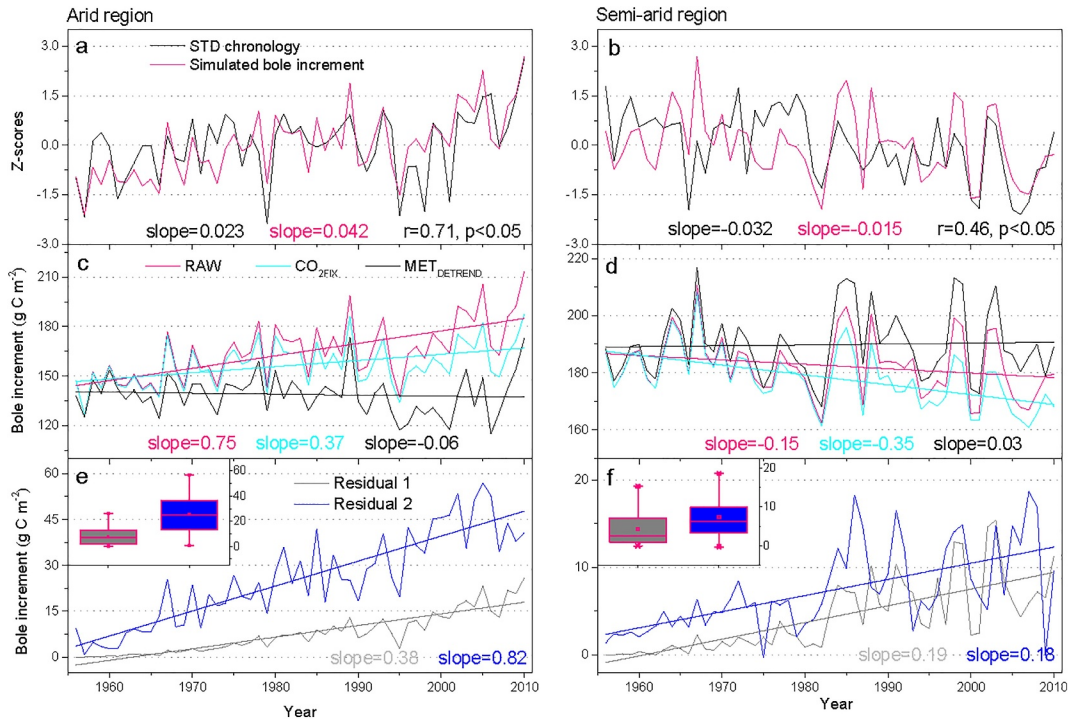

Figure 3. Comparison between measured tree-ring width and simulated bole increment in the arid and semi-arid regions during the period 1956–2010 (a, b). Simulated bole increment with three experiments (c, d). Simulated bole increment was caused by increasing CO_2 concentration (Residual 1) and climate factors (Residual 2) (e, f). Residual 1: RAW minus CO_{2FIX}. Residual 2: RAW minus $MET_{DETREND}$. Inset: distributions of bole increment (Residual 1 and Residual 2 series). To be comparable, the sign of the Residual 2 series in the semi-arid region was reversed.

3.2. Diagnosing Climatic Drivers of Tree Growth Trends

The bole increment trends caused by climatic trends (Residual 2 series) can be separated into two parts: extension of growing season length (Extra length series, Figures 4c and 4d), and changes of daily NPP (Net Primary Productivity) allocated to the tree stem (Drought series, Figures 4c and 4d). According to the MAIDENiso model output, the warming trend of mean annual temperature (Figure 2) lengthened the growing season, and its average length increased from 69 to 92 days in RAW for the arid region, and from 102 to 106 days in the semi-arid region (Figures 4a and 4b). The prolonged growing season length has a positive effect on simulated tree growth, but it is outweighed by the changes in the amount of daily stem NPP (Figures 4c and 4d). The slopes of bole increment resulting from growing season elongation and the amount of daily stem NPP were 0.32 and 0.50 g C m^{-2} yr^{-1} in the arid region, respectively. Correspondingly, those slopes were 0.06 and −0.25 g C m^{-2} yr^{-1} in the semi-arid region, respectively (Figures 4c and 4d). Furthermore, the average increase of bole increment attributed to growing season elongation and to changes in the amount of daily stem NPP were 9.39 and 16.31 g C m^{-2} in the arid region, and 1.69 and −9.04 g C m^{-2} in the semi-arid region (Figures 4e and 4f).

As simulated in MAIDENiso, climatic factors had significant influences on a water stress function, ranging from 0 (maximum stress) to 1 (no stress), and on stomatal conductance in both regions (Figure S8 in Supporting Information S1). We found that stomatal conductance explained over 60% of the variance in bole increment and was closely linked to water stress (Figure S9 in Supporting Information S1). Stomatal conductance increased with the relief of water stress, resulting in an improvement of NPP. The increase of CO_2 had a slight positive effect on photosynthetic rate and, therefore, induced a relatively small increase in NPP (compare RAW and CO_{2FIX} in Figures S8 and S10 in Supporting Information S1). Larger differences in NPP were found between RAW and $MET_{DETREND}$. In the arid region, the water stress function was closer to zero (closer to maximum water stress) and stomatal conductance was strongly reduced in $MET_{DETREND}$ compared to RAW, resulting in a significant decrease in NPP (Figures S8a, S8e, and S8g in Supporting Information S1). In the semi-arid region, by contrast,

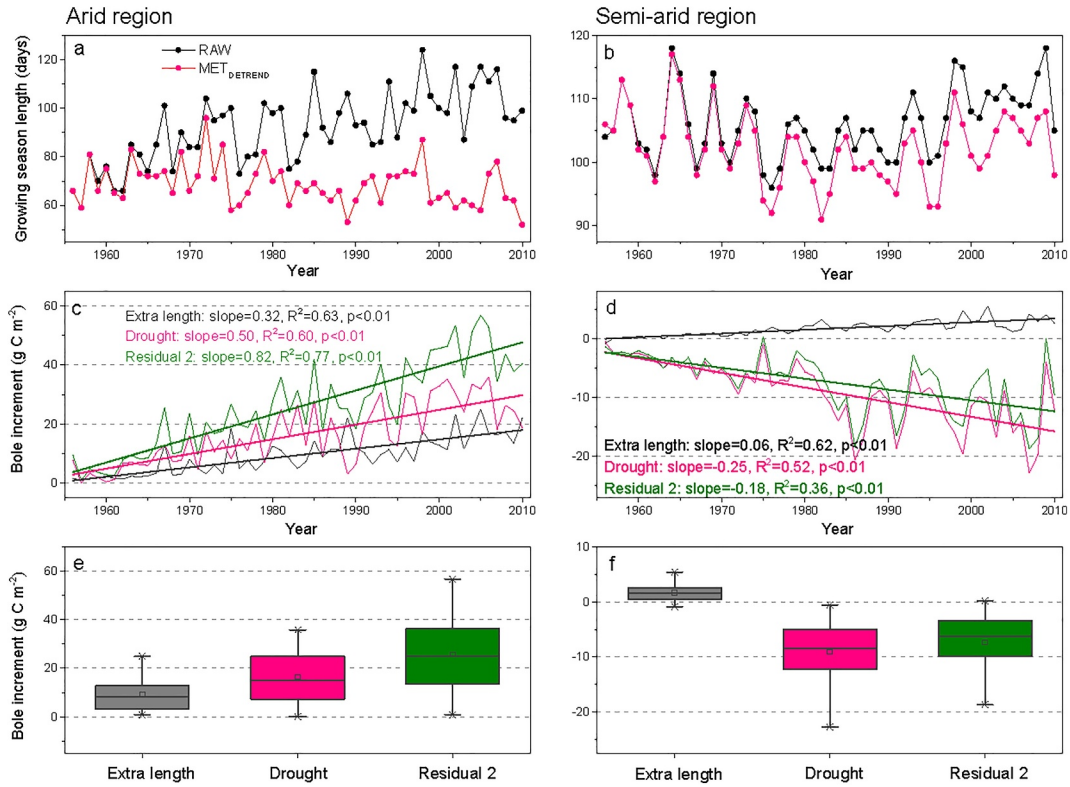

Figure 4. Variations of growing season length simulated by MAIDENiso RAW and $MET_{DETREND}$ experiments (a–d) Changes of bole increment. Residual 2: RAW minus $MET_{DETREND}$ simulated bole increment; Extra length: bole increment due to extended growing days; Drought: bole increment due to changed daily carbon allocated to tree stem, estimated as Residual 2 minus Extra length series (e, f). Distributions of bole increment corresponding to the series in panels (c, d).

$MET_{DETREND}$ yielded a higher water stress function value, therefore increasing stomatal conductance and NPP (Figures S8b, S8f, and S8h in Supporting Information S1).

3.3. Long-Term Variations of C_i, C_i/C_a and iWUE Derived From Tree-Ring $\delta^{13}C$

As atmospheric CO_2 increases, an overall accelerating trend of intercellular CO_2 (C_i) was modeled from stable carbon isotope in both study regions since the year 1900 (Figures 5e and 5f). Before 1950, the intercellular CO_2 decreased slightly in the arid region, and increased in the semi-arid region. This resulted in decreases in C_i/C_a because of the increase in atmospheric CO_2. After 1950, C_i/C_a shows a significant increasing trend (slope = 0.0006 yr^{-1}, $P < 0.01$) in the arid region but a significant decreasing trend (slope = −0.0008 yr^{-1}, $P < 0.01$) in the semi-arid region (Figures 5c and 5d). The mean iWUE over 1900–2010 was greater in the arid region (141.3 μmol mol^{-1}) than the semi-arid region (102.4 μmol mol^{-1}). Furthermore, iWUE exhibited a significant upward trend since 1900 in both regions, related primarily to the increased atmospheric CO_2 but modified by opposite trends in C_i/C_a (Equation 1) in the two regions after 1950. Therefore, iWUE in the arid region increased by 29% over 1900–2010 (with a slight positive trend before 1950, 0.24 μmol mol^{-1} yr^{-1}, then increased to 0.44 μmol mol^{-1} yr^{-1} since 1950) while it increased by 44% in the semi-arid region, at a rate of 0.13 and 0.62 μmol mol^{-1} yr^{-1} before and after the year 1950 (Figures 5a and 5b). Within the arid region, observed iWUE can be associated with a constant C_i scenario (Figure S11 in Supporting Information S1). Except that in the semi-arid region where this approximation underpredicts iWUE after 1985 (Figure S11 in Supporting Information S1) because measured C_i/C_a falls below its mean value (Figure 5d). Furthermore, we employed fitted equations to establish a linear relationship between tree growth and iWUE. The results revealed a positive correlation between radial growth and iWUE in arid region, whereas a negative correlation was observed in semi-arid region, where tree radial growth declined with increasing iWUE (Figure S12 in Supporting Information S1).

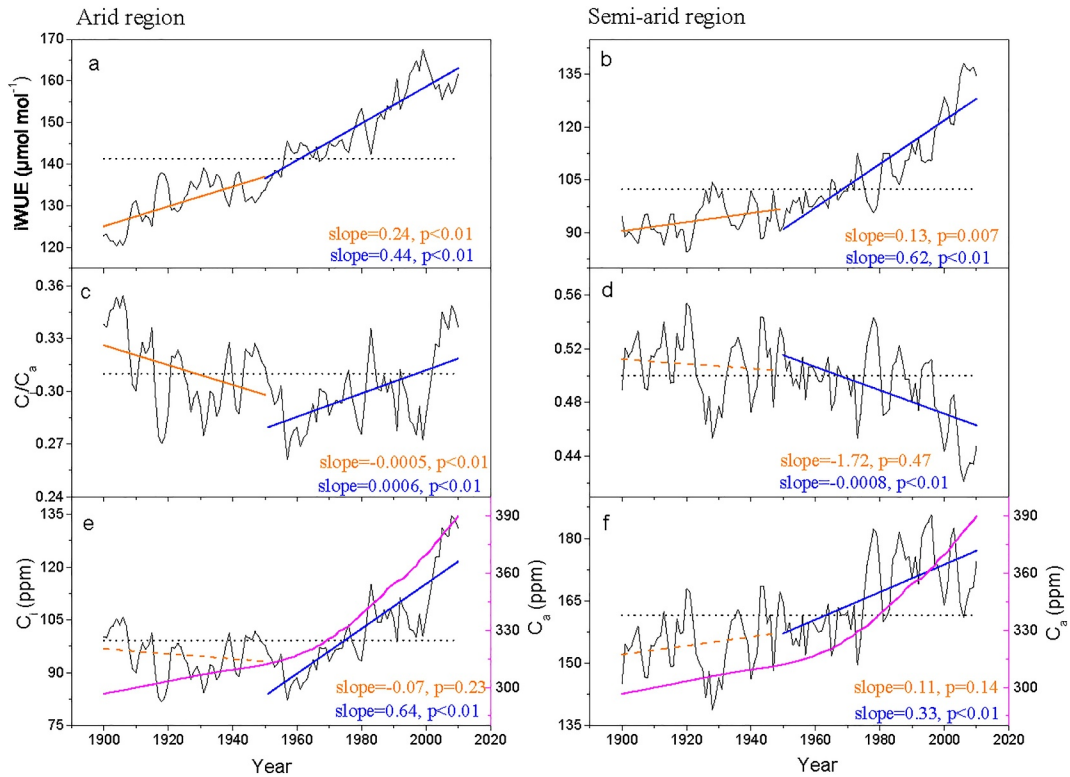

Figure 5. Variations of tree physiological parameters in arid and semi-arid regions during the period 1900–2010. The linear trends were shown in two sub-periods (1900–1950 with yellow line and 1950–2010 with blue line) for iWUE (a, b), C_i/C_a (c, d) and C_i (e, f). The dotted black lines are the mean values of the corresponding parameters over the whole period. Non-significant (significant) linear trends are dashed (solid) lines. The pink line (e, f) is atmospheric CO_2 concentration (ppm, right-hand scale).

4. Discussion

We present empirical and mechanistic evidence that trees adjusted their metabolism in arid and semi-arid regions of China under increasing CO_2 and climate change since the 1950s. A key finding is that, compared with the effect of climate on tree growth, the positive effect of increased atmospheric CO_2 since the 1950s was rather small, the slopes and mean values of the residual series (Figure 3), indicating that climate acts as the main driver in controlling tree growth rather than atmospheric CO_2 concentration. Rezsöhazy et al. (2021) have used the MAIDEN model to simulate tree-ring width chronologies on global scale, which include 64 sampling sites mainly distributed in Asia, Europe, and North America. The sensitivity analysis of MAIDEN to atmospheric CO_2 concentration showed that the simulated growth is closer to the observed tree-ring width when including the increase in CO_2 concentration, which is similar to the results of our study, and also indicate its potential advantage over statistical and simple process-based models. In the three scenarios, we had compared the same parameters except for different input data in each study region. This might cause some deviations in the trends caused by carbon dioxide and climatic factors. However, similar results were found in a boreal coniferous forest in Southern Finland based on 17 years' eddy-covariance measurements, which showed that only 30%–40% of the observed increase in ecosystem GPP could be attributed to CO_2 (Launiainen et al., 2022). For now, although atmospheric CO_2 had reached 390 ppm by the end of our analysis period, it still did not meet the demands of carbon assimilation for most C_3 plants (Jiang et al., 2004). Previous studies found photosynthetic enhancement of trees by elevated CO_2 (Long, 1991; Quentin et al., 2015). Therefore, the small increased net productivity in our study regions (Residual 1 in Figure 3) was likely caused by an increase in carbon assimilation under increased CO_2.

Climate can have an important impact on tree growth, either by changing growing season length, or by changing the NPP on days during the growing season and its allocation to different tree compartments. The growing season length modeled from MAIDENiso was significantly extended (Figure 4), namely an earlier start of the growing season, which was triggered by rising temperature in both regions. A previous study (Yang et al., 2017)

demonstrated that temperature had an important effect on the beginning of the growing season over the Tibetan Plateau. Also, from the perspective of a micro-coring experiment, Ren et al. (2018) found that xylem phenology on the northeastern Tibetan Plateau can start only when both critical temperature and precipitation thresholds are reached during spring. Our results from the arid and semi-arid regions showed that the increased tree growth caused by a lengthening of the growing season was quite small (Figure 4), suggesting that the increase in tree growth was mainly due to the intra-annual variation of climate. We think that water stress was the most important factor affecting tree productivity through regulation of leaf conductance (Figure S8 and S9 in Supporting Information S1). When water stress becomes severe, trees prefer to close their stomata in order to reduce the water loss through transpiration, thus reducing photosynthetic activity. A reduction in stomatal conductance was modeled in the arid region for trees experiencing a more xeric condition (compared with RAW, $MET_{DETREND}$ represents a relative xeric condition). In contrast, higher productivity was modeled when water stress was alleviated in the semi-arid region (Figure S10 in Supporting Information S1). The significant downward trend of tree growth in the semi-arid region was therefore to a large extent closely related to drought condition. The MAIDENiso model has great advantages to explore the effects of climate factors and increasing atmospheric carbon dioxide concentration on the radial growth of trees. However, other factors still neglected by the model, such as nutrient supply and interspecific competition, could play a role in tree growth and should be considered in successive studies.

Studies based on large data sets have found increases in iWUE across wide spatial scales (Adams et al., 2020; Keenan et al., 2013; Panthi et al., 2019; Peñuelas et al., 2011). The increase in iWUE at our sites is comparable with the global average iWUE increase (20.5%) (Peñuelas et al., 2011), with respective rates of 16.9% and 30.3% in the arid and semi-arid regions from 1960 to 2000. As atmospheric CO_2 concentration has increased since 1850, one could expect forests to benefit from a CO_2 fertilization effect (Wang et al., 2019). However, some studies found nonsignificant increase in tree growth as atmospheric CO_2 concentration and iWUE rose (Giguère-Croteau et al., 2019; Panthi et al., 2019; Sleen et al., 2015). The significant increase in iWUE is related to a proportional adjustment between CO_2 assimilation rate and stomatal conductance. Based on MAIDENiso model outputs, we conclude that the impact of reduced stomatal conductance on tree growth is much more important than the slightly increased photosynthetic rate resulting from elevated CO_2, which was confirmed by the close relationship between iWUE and a constant C_i/C_a scenario after 1950 (Figure S11 in Supporting Information S1), indicating that the increased iWUE in our study regions may not stimulate growth in the tree stem. This is likely why tree growth did not match increases in iWUE in the semi-arid region (Figure S12 in Supporting Information S1). Such climate-modulated stomatal responses were also found in previous studies (Guerrieri et al., 2019; Panthi et al., 2019; Wang et al., 2012).

5. Conclusion

The use of the process-based ecophysiological model MAIDENiso was specifically appropriate for analyzing the response of increment in radial growth to climate and CO_2 concentration from a mechanistic perspective. Comparing the slopes and mean values of the residual series, we found that bole increment changes caused by climatic trends were larger than expected if caused only by increased CO_2. Results highlighted that climate acts as the main driver controlling growth in the tree boles. That is, water stress rather than CO_2 increases or prolonged growing seasons dominates tree stem growth and trends in our study regions. Moreover, based on tree-ring $\delta^{13}C$ records, we found that the increased iWUE was caused by an enhanced carbon assimilation rate. Drought stress could offset the beneficial effects provided by elevated CO_2, namely living trees will not capture more carbon as long as growth remains limited by dry climate conditions. However, our study did not consider other factors of the model, such as competition and nutrient limitation, which may also influence tree growth (Gruber & Galloway, 2008). The current model version does not account for the effects of snowmelt on tree growth, despite the evidence provided in the literature (Danis et al., 2012; Hagedorn et al., 2014; Wu et al., 2019; Zhang et al., 2016). This limitation may introduce potential biases into our findings. Improvement of the physiological processes in MAIDENiso including additional biotic and abiotic factors would provide more flexibility for investigating tree growth and future forest dynamics in response to global change on a large scale.

Conflict of Interest

The authors declare no conflicts of interest relevant to this study.

Data Availability Statement

Meteorological observations were obtained from the China National Meteorological Science Data Center (https://data.cma.cn/dataService/cdcindex/datacode/A.0012.0001/show_value/normal.html). Atmospheric CO_2 concentration records were obtained from the Mauna Loa Observatory (https://gml.noaa.gov/ccgg/trends/data.html). The CN05.1 gridded data set is available from Wang (2025) via figshare (https://doi.org/10.6084/m9.figshare.28702061.v1). The ERA5-Land reanalysis data set was obtained from the Copernicus Climate Data Store (Copernicus Climate Change Service, 2022; https://cds.climate.copernicus.eu/datasets/reanalysis-era5-land-monthly-means). SPEI data were obtained through the KNMI climate explorer ((Trouet & Van Oldenborgh, 2013; http://climexp.knmi.nl). Reconstructed PDSI data were obtained from Cook et al. (2010) (https://www.ncei.noaa.gov/pub/data/paleo/treering/reconstructions/asia/cook2010pdsi/). Tree-ring width chronologies and tree-ring $\delta^{13}C$ chronologies generated in this study are available from the corresponding author upon reasonable request. Eddy covariance data from the Dayekou Guantan forest station are available at https://eco.gssdc.cn/metadata/b87808ab-5c18-4096-863d-12a447f24016.

Acknowledgments
The climate data were obtained from the weather information center of the China Meteorological Administration. B.Y., T.Y. and J.W. are funded by the National Natural Science Foundation of China (NSFC) (Grants 42130511 and 42261134537). We are grateful the Shaanxi Natural Science Foundation Project (2022JQ-257). B.Y., T.Y., and T.J. O. were supported by the Belmont Forum and JPI-Climate, Collaborative Research Action "INTEGRATE, an integrated data-model study of interactions between tropical monsoons and extratropical climate variability and extremes" (NSFC Grant 41661144008; NERC Grant NE/P006809/1). All data presented in this article will be freely accessible (https://www.ncdc.noaa.gov/paleo/) after publication.

References

Adams, M. A., Buckley, T. N., & Turnbull, T. L. (2020). Diminishing CO_2-driven gains in water-use efficiency of global forests. *Nature Climate Change*, *10*(5), 466–471. https://doi.org/10.1038/s41558-020-0747-7

Ainsworth, E. A., & Long, S. P. (2005). What have we learned from 15 years of free-air CO_2 enrichment (FACE)? A meta-analytic review of the responses of photosynthesis, canopy properties and plant production to rising CO_2. *New Phytologist*, *165*(2), 351–372. https://doi.org/10.1111/j.1469-8137.2004.01224.x

Ainsworth, E. A., & Rogers, A. (2007). The response of photosynthesis and stomatal conductance to rising [CO_2]: Mechanisms and environmental interactions. *Plant, Cell and Environment*, *30*(3), 258–270. https://doi.org/10.1111/j.1365-3040.2007.01641.x

Babst, F., Alexander, M. R., Szejner, P., Bouriaud, O., Klesse, S., Roden, J., et al. (2014). A tree-ring perspective on the terrestrial carbon cycle. *Oecologia*, *176*(2), 307–322. https://doi.org/10.1007/s00442-014-3031-6

Cernusak, L. A., Winter, K., Dalling, J. W., Holtum, J. A. M., Jaramillo, C., Körner, C., et al. (2013). Tropical forest responses to increasing atmospheric CO_2: Current knowledge and opportunities for future research. *Functional Plant Biology*, *40*(6), 531–551. https://doi.org/10.1071/FP12309

Cook, E. R. (1985). *A time-series analysis approach to tree-ring standardization* [Doctoral Dissertation]. University of Arizona. Retrieved from https://www.st-andrews.ac.uk/~rjsw/PalaeoPDFs/Cook1985-Chapter%202.pdf.(.

Cook, E. R., Anchukaitis, K. J., Buckley, B. M., D'Arrigo, R. D., Jacoby, G. C., & Wright, W. E. (2010). Asian monsoon failure and megadrought during the last millennium. *Science*, *328*(5977), 486–489. https://doi.org/10.1126/science.1185188

Copernicus Climate Change Service. (2022). ERA5-Land monthly averaged data from 1950 to present. *Copernicus Climate Change Service (C3S) Climate Data Store (CDS)*. https://doi.org/10.24381/cds.68d2bb30

Danis, P. A., Hatté, C., Misson, L., & Guiot, J. (2012). MAIDENiso: A multiproxy biophysical model of tree-ring width and oxygen and carbon isotopes. *Canadian Journal of Forest Research*, *42*(9), 1697–1713. https://doi.org/10.1139/X2012-089

Farquhar, G. D., O'Leary, M. H., & Berry, J. A. (1982). On the relationship between carbon isotope discrimination and the intercellular carbon dioxide concentration in leaves. *Australian Journal of Plant Physiology*, *9*(2), 121–137. https://doi.org/10.1071/PP9820121

Flato, G., Marotzke, J., Abiodun, B., Braconnot, P., Chou, S. C., C ollins, W. J., et al. (2013). Evaluation of climate models. In *In climate change 2013: The physical science basis. Contribution of working group I to the fifth assessment report of the intergovernmental panel on climate change* (pp. 95–123). Cambridge University press.

Gao, J., Rossi, S., & Yang, B. (2021). Origin of intra-annual density fluctuations in a semi-arid area of Northwestern China. *Frontiers of Plant Science*, *12*, 777753. https://doi.org/10.3389/fpls.2021.777753

Gea-Izquierdo, G., Guibal, F., Joffre, R., Ourcival, J. M., Simioni, G., & Guiot, J. (2015). Modelling the climatic drivers determining photosynthesis and carbon allocation in evergreen Mediterranean forests using multiproxy long time series. *Biogeosciences*, *12*(12), 3695–3712. https://doi.org/10.5194/bg-12-3695-2015

Gennaretti, F., Gea-Izquierdo, G., Boucher, E., Berninger, F., Arseneault, D., & Guiot, J. (2017). Ecophysiological modeling of photosynthesis and carbon allocation to the tree stem in the boreal forest. *Biogeosciences*, *14*(21), 4851–4866. https://doi.org/10.5194/bg-14-4851-2017

Giguère-Croteau, C., Boucher, É., Bergeron, Y., Girardin, M. P., Drobyshev, I., Silva, L. C. R., et al. (2019). North America's oldest boreal trees are more efficient water users due to increased [CO_2], but do not grow faster. *Proceedings of the national academy of sciences* (Vol. 116(7), pp. 2749–2754). https://doi.org/10.1073/pnas.1816686116

Girardin, M. P., Bouriaud, O., Hogg, E. H., Kurz, W., Zimmermann, N. E., Metsaranta, J. M., et al. (2016). No growth stimulation of Canada's boreal forest under half-century of combined warming and CO_2 fertilization. *Proceedings of the national academy of sciences* (Vol. 113(52), pp. E8406–E8414). https://doi.org/10.1073/pnas.1610156113

Gruber, N., & Galloway, J. N. (2008). An Earth-System perspective of the global nitrogen cycle. *Nature*, *451*(7176), 293–296. https://doi.org/10.1038/nature06592

Guerrieri, R., Belmecheri, S., Ollinger, S. V., Asbjornsen, H., Jennings, K., Xiao, J., et al. (2019). Disentangling the role of photosynthesis and stomatal conductance on rising forest water-use efficiency. *Proceedings of the national academy of sciences of the United States of America* (Vol. 116(34), pp. 16909–16914). https://doi.org/10.1073/pnas.1905912116

Hagedorn, F., Shiyatov, S. G., Mazepa, V., Devi, N., Grigor'ev, A. A., Bartysh, A. A., et al. (2014). Treeline advances along the Urals Mountain range-driven by improved winter conditions? *Global Change Biology*, *20*(11), 3530–3543. https://doi.org/10.1111/gcb.12613

Harsch, M. A., Hulme, P. E., McGlone, M. S., & Duncan, R. P. (2009). Are treelines advancing? A global meta-analysis of treeline response to climate warming. *Ecology Letters*, *12*(10), 1040–1049. https://doi.org/10.1111/j.1461-0248.2009.01355.x

Holmes, R. L. (1983). Computer-assisted quality control in tree-ring dating and measurement. *Tree-Ring Bulletin*, *43*, 69–78. http://hdl.handle.net/10150/261233

Huang, R., Zhu, H., Liu, X., Liang, E., Grießinger, J., Bräuning, A., et al. (2016). Does increasing intrinsic Water Use Efficiency (iWUE) stimulate tree growth at natural alpine timberline on the southeastern Tibetan Plateau? *Global and Planetary Change*, *148*, 217–226. https://doi.org/10.1016/j.gloplacha.2016.11.017

Jiang, G., Chan, J., Gao, Y., & Li, Y. (2004). *Plant ecophysiology*. Higher Education Press.

Keenan, T. F., Hollinger, D. Y., Bohrer, G., Dragoni, D., Munger, J. W., Schmid, H. P., & Richardson, A. D. (2013). Increase in forest water-use efficiency as atmospheric carbon dioxide concentrations rise. *Nature*, *499*(7458), 324–327. https://doi.org/10.1038/nature12291

Launiainen, S., Katul, G. G., Leppä, K., Kolari, P., Aslan, T., Grönholm, T., et al. (2022). Does growing atmospheric CO_2 explain increasing carbon sink in a boreal coniferous forest? *Global Change Biology*, *28*(9), 2910–2929. https://doi.org/10.1111/gcb.16117

Lavergne, A., Voelker, S., Csank, A., Graven, H., Boer, H. J., Daux, V., et al. (2019). Historical changes in the stomatal limitation of photosynthesis: Empirical support for an optimality principle. *New Phytologist*, *225*(6), 2484–2497. https://doi.org/10.1111/nph.16314

Liang, E., Liu, X., Yuan, Y., Qin, N., Fang, X., Huang, L., et al. (2006). The 1920s drought recorded by tree rings and historical documents in the semi-arid and arid areas of northern China. *Climatic Change*, *79*(3–4), 403–432. https://doi.org/10.1007/s10584-006-9082-x

Long, S. P. (1991). Modification of the response of photosynthetic productivity to rising temperature by atmospheric CO_2 concentrations: Has its importance been underestimated? *Plant, Cell and Environment*, *14*(8), 729–739. https://doi.org/10.1111/j.1365-3040.1991.tb01439.x

Marchand, W., Girardin, M. P., Hartmann, H., Depardieu, C., Bergeron, Y., Gauthier, S., et al. (2020). Strong overestimation of water-use efficiency responses to rising CO_2 in tree-ring studies. *Global Change Biology*, *26*(8), 4538–4558. https://doi.org/10.1111/gcb.15166

McCarroll, D., & Loader, N. J. (2004). Stable isotopes in tree rings. *Quaternary Science Reviews*, *23*(7–8), 771–801. https://doi.org/10.1016/j.quascirev.2003.06.017

Misson, L. (2004a). A model for analyzing ecosystem processes in dendroecology. *Canadian Journal of Forest Research*, *34*(4), 874–887. https://doi.org/10.1139/X03-252

Misson, L. (2004b). MAIDEN: A model to analyze ecosystem processes in dendroecology. *Canadian Journal of Forest Research*, *34*(4), 874–887. https://doi.org/10.1139/X03-252

Muñoz Sabater, J. (2019). ERA5-Land monthly averaged data from 1950 to present. *Copernicus Climate Change Service (C3S) Climate Data Store (CDS)*. https://doi.org/10.24381/cds.68d2bb30

Pan, Y., Birdsey, R. A., Fang, J., Houghton, R., Kauppi, P. E., Kurz, W. A., et al. (2011). A large and persistent carbon sink in the world's forests. *Science*, *333*(6045), 988–993. https://doi.org/10.1126/science.1201609

Panthi, S., Fan, Z., Sleen, V. P., & Zuidema, P. A. (2019). Long-term physiological and growth responses of Himalayan fir to environmental change are mediated by mean climate. *Global Change Biology*, *26*(3), 1778–1794. https://doi.org/10.1111/gcb.14910

Peng, X., Du, J., Yang, B., Xiao, S., & Li, G. (2019). Elevation-influenced variation in canopy and stem phenology of Qinghai spruce, central Qilian Mountains, northeastern Tibetan Plateau. *Trees*, *33*(3), 707–717. https://doi.org/10.1007/s00468-019-01810-z

Peñuelas, J., Canadell, J. G., & Ogaya, R. (2011). Increased water-use efficiency during the 20th century did not translate into enhanced tree growth. *Global Ecology and Biogeography*, *20*(4), 597–608. https://doi.org/10.1111/j.1466-8238.2010.00608.x

Qin, C., Yang, B., Bräuning, A., Ljungqvist, F. C., Osborn, T. J., Shishov, V., et al. (2025). Persistent humid climate favored the Qin and Western Han Dynasties in China around 2200 y ago. *Proceedings of the national academy of sciences* (Vol. 122(1), p. e2415294121). https://doi.org/10.1073/pnas.2415294121

Quentin, A. G., Crous, K. Y., Barton, C. V. M., & Ellsworth, D. S. (2015). Photosynthetic enhancement by elevated CO_2 depends on seasonal temperatures for warmed and non-warmed Eucalyptus globulus trees. *Tree Physiology*, *35*(11), 1249–1263. https://doi.org/10.1093/treephys/tpv110

Ren, P., Rossi, S., Camarero, J. J., Ellison, A. M., Liang, E., & Peñuelas, J. (2018). Critical temperature and precipitation thresholds for the onset of xylogenesis of Juniperus przewalskii in a semi-arid area of the north-eastern Tibetan Plateau. *Annals of Botany*, *121*(4), 617–624. https://doi.org/10.1093/aob/mcx188

Rezsöhazy, J., Gennaretti, F., Goosse, H., & Guiot, J. (2021). Testing the performance of dendroclimatic process-based models at global scale with the PAGES2k tree-ring width database. *Climate Dynamics*, *57*(7–8), 2005–2020. https://doi.org/10.1007/s00382-021-05789-7

Saurer, M., Siegwolf, R. T. W., & Schweingruber, F. H. (2004). Carbon isotope discrimination indicates improving water-use efficiency of trees in northern Eurasia over the last 100 years. *Global Change Biology*, *10*(12), 2109–2120. https://doi.org/10.1111/j.1365-2486.2004.00869.x

Silva, L. C. R., Geng, S., Xia, Z. B., Liang, Q., Ning, W., & Horwath, W. R. (2016). Tree growth acceleration and expansion of alpine forests: The synergistic effect of atmospheric and edaphic change. *Science Advances*, *2*(8), e1501302. https://doi.org/10.1126/sciadv.1501302

Sleen, V. P., Groenendijk, P., Vlam, M., Anten, N. P. R., Boom, A., Bongers, F., et al. (2015). No growth stimulation of tropical trees by 150 years of CO_2 fertilization but water-use efficiency increased. *Nature Geoscience*, *8*(1), 24–28. https://doi.org/10.1038/NGEO2313

Stokes, M. A., & Smiley, T. L. (1968). *An introduction to tree-ring dating*. University of Chicago Press.

Tolwinski-Ward, S. E., Evans, M. N., Hughes, M. K., & Anchukaitis, K. J. (2010). An efficient forward model of the climate controls on interannual variation in tree-ring width. *Climate Dynamics*, *36*(11–12), 2419–2439. https://doi.org/10.1007/s00382-010-0945-5

Trouet, V., & Van Oldenborgh, G. J. (2013). KNMI climate explorer: A web-based research tool for high-resolution paleoclimatology. *Tree-Ring Research*, *69*(1), 3–13. https://doi.org/10.3959/1536-1098-69.1.3

Wang, H. (2025). CN05.1 dataset. https://doi.org/10.6084/m9.figshare.28702061.v1

Wang, W., Liu, X., An, W., Xu, G., & Zeng, X. (2012). Increased intrinsic water-use efficiency during a period with persistent decreased tree radial growth in northwestern China: Causes and implications. *Forest Ecology and Management*, *275*, 14–22. https://doi.org/10.1016/j.foreco.2012.02.027

Wang, W., Liu, X., Xu, G., Treydte, K., Shao, X., Qin, D., et al. (2019). CO_2 fertilization confounds tree-ring records of regional hydroclimate at northeastern Qinghai-Tibetan Plateau. *Earth and Space Science*, *6*(5), 730–740. https://doi.org/10.1029/2018ea000529

Wieloch, T., Helle, G., Heinrich, I., Voigt, M., & Schyma, P. (2011). A novel device for batch-wise isolation of α-cellulose from small-amount wholewood samples. *Dendrochronologia*, *29*(2), 115–117. https://doi.org/10.1016/j.dendro.2010.08.008

Williams, A. P., Allen, C. D., Macalady, A. K., Griffin, D., Woodhouse, C. A., Meko, D. M., et al. (2013). Temperature as a potent driver of regional forest drought stress and tree mortality. *Nature Climate Change*, *3*, 292–297. https://doi.org/10.1038/NCLIMATE1693

Wu, C., & Xing, C. (2015). Comparison of fine root biomass of three main arbors in Qilian Mountains. *Research of Soil and Water Conservation*, *22*(5), 325–330. (in Chinese). https://doi.org/10.13869/j.cnki.rswc.2015.05.059

Wu, J., & Gao, X. (2013). A gridded daily observation dataset over China region and comparison with the other datasets (in Chinese). *Chinese Journal of Geophysics*, *56*(4), 1102–1111.

Wu, X. C., Li, X. Y., Liu, H. Y., Ciais, P., Li, Y. Q., Xu, C. Y., et al. (2019). Uneven winter snow influence on tree growth across temperate China. *Global Change Biology*, *25*(1), 144–154. https://doi.org/10.1111/gcb.14464

Yang, B., He, M., Shishov, V., Tychkov, I., Vaganov, E., Rossi, S., et al. (2017). New perspective on spring vegetation phenology and global climate change based on Tibetan Plateau tree-ring data. *Proceedings of the national academy of sciences* (Vol. 114(27), pp. 6966–6971). https://doi.org/10.1073/pnas.1616608114

Yang, B., He, M. H., Yang, L., Wang, F., & Ljungqvist, F. C. (2023). Pine maximum latewood density in semi-arid Northern China records hydroclimate rather than temperature. *Geophysical Research Letters*, *50*(13), e2023GL104362. https://doi.org/10.1029/2023gl104362

Yang, B., Kang, S., Ljungqvist, F. C., He, M., Zhao, Y., & Qin, C. (2014). Drought variability at the northern fringe of the Asian summer monsoon region over the past millennia. *Climate Dynamics*, *43*(3–4), 845–859. https://doi.org/10.1007/s00382-013-1962-y

Yang, B., Qin, C., Wang, J., He, M., Melvin, T. M., Osborn, T. J., & Briffa, K. R. (2014). A 3,500-year tree-ring record of annual precipitation on the northeastern Tibetan Plateau. *Proceedings of the national academy of sciences* (Vol. 111(8), pp. 2903–2908). https://doi.org/10.1073/pnas.1319238111

Zeng, Q., Rossi, S., & Yang, B. (2017). Effects of age and size on xylem phenology in two conifers of Northwestern China. *Frontiers in Plant Science*, *8*, 2264. https://doi.org/10.3389/fpls.2017.02264

Zhang, X. L., Bai, X. P., Chang, Y. X., & Chen, Z. J. (2016). Increased sensitivity of Dahurian larch radial growth to summer temperature with the rapid warming in Northeast China. *Trees*, *30*(5), 1799–1806. https://doi.org/10.1007/s00468-016-1413-6

Zhao, C., Shen, W., & Peng, H. (2009). Methods for determining canopy leaf area index of Picea crassifolia forest in Qilian Mountains, China. *Chinese Journal of Plant Ecology*, *33*(5), 860–869. https://doi.org/10.3773/j.issn.1005-264x.2009.05.004

Zheng, J., Bian, J., Ge, Q., & Yin, Y. (2013). The climate regionalization in China for 1951–1980 and 1981–2010 (in Chinese). *Geographical Research*, *32*(6), 987–997. https://doi.org/10.11821/yj2013060002

Zuidema, P. A., Heinrich, I., Rahman, M., Vlam, M., Zwartsenberg, S. A., & Sleen, V. P. (2020). Recent CO_2 rise has modified the sensitivity of tropical tree growth to rainfall and temperature. *Global Change Biology*, *26*(1), 4028–4041. https://doi.org/10.1111/gcb.15092

References From the Supporting Information

Cai, Q., Liu, Y., Lei, Y., Bao, G., & Sun, B. (2014). Reconstruction of the March-August PDSI since 1703 AD based on tree rings of Chinese pine (Pinus tabulaeformis Carr.) in the Lingkong Mountain, southeast Chinese Loess Plateau. *Climate of the Past*, *10*(2), 509–521. https://doi.org/10.5194/cp-10-509-2014

Chen, L., Guo, K., Gou, X., Zhao, X., & Ma, H. (2025). Community components and characteristics of Juniperus przewalskii forests (in Chinese). *Chinese Journal of Plant Ecology*, *49*. https://doi.org/10.17521/cjpe.2024.0163

De Pury, D. G. G., & Farquhar, G. D. (1997). Simple scaling of photosynthesis from leaves to canopies without the errors of big-leaf models. *Plant, Cell and Environment*, *20*(5), 537–557. https://doi.org/10.1111/j.1365-3040.1997.00094.x

Deng, Y., Gou, X., Gao, L., Zhang, F., Xu, X., & Yang, M. (2016). Tree-ring recorded drought variability in the northern Min Mountains of northwestern China. *International Journal of Climatology*, *36*(10), 3550–3560. https://doi.org/10.1002/joc.4575

Fang, K., Gou, X., Chen, F., D'Arrigo, R., & Li, J. (2009). Tree-ring based drought reconstruction for the Guiqing Mountain (China): Linkages to the Indian and Pacific Oceans. *International Journal of Climatology*, *30*(8), 1137–1145. https://doi.org/10.1002/joc.1974

Guo, K., Fang, J., Wang, G., Tang, Z., Xie, Z., Shen, Z., et al. (2020). A revised scheme of vegetation classification system of China (in Chinese). *Chinese Journal of Plant Ecology*, *44*(2), 111–127. https://doi.org/10.17521/cjpe.2019.0271

Guo, Q., Xu, D., & Yan, H. (1995). A study on the impacts of climate change on the distribution of Pinus tabulae formis in China (in Chinese). *Scientia Silvae Sinicae*, *31*(5), 393–402.

Leuning, R. (1995). A critical appraisal of a combined stomatal photosynthesis model for C_3 plants. *Plant, Cell and Environment*, *18*(4), 339–355. https://doi.org/10.1111/j.1365-3040.1995.tb00370.x

Li, J., Chen, F., Cook, E. R., Gou, X., & Zhang, Y. (2007). Drought reconstruction for North Central China from tree rings: The value of the palmer drought severity index. *International Journal of Climatology*, *27*(7), 903–909. https://doi.org/10.1002/joc.1450

Liu. (1962). The development of sandy soil in the Qaidam Basin (in Chinese). *Chinese Journal of Soil Science*, *4*(9), 45–48. https://doi.org/10.19336/j.cnki.trtb.1962.04.009

Nimon, K., Lewis, M., Kane, R., & Haynes, R. M. (2008). An R package to compute commonality coefficients in the multiple regression case: An introduction to the package and a practical example. *Behavior Research Methods*, *40*(2), 457–466. https://doi.org/10.3758/brm.40.2.457

Sheppard, P. R., Tarasov, P. E., Graumlich, L. J., Heussner, K. U., Wagner, M., Österle, H., & Thompson, L. G. (2004). Annual precipitation since 515 BC reconstructed from living and fossil juniper growth of northeastern Qinghai Province, China. *Climate Dynamics*, *23*(7), 869–881. https://doi.org/10.1007/s00382-004-0473-2

Wu, G., & Feng, Z. (1994). Study on the social characteristics and biomass of the Pinus tabulae formis forest systems in China (in Chinese). *Acta Ecologica Sinica*, *14*(4), 416–422.

Yang, B., Qin, C., Shi, F., & Sonechkin, D. M. (2012). Tree ring-based annual streamflow reconstruction for the Heihe River in arid northwestern China from AD575 and its implications for water resource management. *The Holocene*, *22*(7), 773–784. https://doi.org/10.1177/0959683611430411

Yang, T., Yang, B., Boucher, É., & Rossi, S. (2021). How did climate and CO_2 concentration affect intrinsic water-use efficiency and tree growth in a semi-arid region of China? *Trees*, *35*(3), 769–781. https://doi.org/10.1007/s00468-020-02075-7

Yang, Y., Ma, Y., Zhao, H., Qi, Y., Zhang, K., & Wang, H. (2021). Soil moisture properties of different climate types in Gansu Province (in Chinese). *Journal of Soil and Water Conservation*, *35*(5), 213–220+226. https://doi.org/10.13870/j.cnki.stbcxb.2021.05.029

Yin, C. (2005). Research on the investigation and control of pests and diseases in Pinus tabulae formis forests of the Qilian Natural Reserve. *Practical Forestry Technology*, *9*, 28–30. https://doi.org/10.13456/j.cnki.lykt.2005.09.017

Zhang, Y., Tian, Q., Gou, X., Chen, F., Leavitt, S. W., & Wang, Y. (2011). Annual precipitation reconstruction since AD 775 based on tree rings from the Qilian Mountains, northwestern China. *International Journal of Climatology*, *31*(3), 371–381. https://doi.org/10.1002/joc.2085